

# Effects of Ultraviolet Absorbers on the Ultraviolet Degradation of Rice-Hull/High-Density Polyethylene Composites

Hua Du,<sup>1,2</sup> Weihong Wang,<sup>1</sup> Qingwen Wang,<sup>1</sup> Shujuan Sui,<sup>1</sup> Yongming Song<sup>1</sup>

<sup>1</sup>Key Laboratory of Bio-Based Material Science and Technology (Ministry of Education), Northeast Forestry University, Harbin 150040, China

<sup>2</sup>Chemistry Department, Harbin Normal University, Harbin 150080, China

Received 2 April 2011; accepted 25 November 2011

DOI 10.1002/app.36558

Published online in Wiley Online Library (wileyonlinelibrary.com).

**ABSTRACT:** In China, rice-hull powder is widely used as a fiber component to reinforce polymers because of its ready availability and lower cost compared to wood fibers. However, an issue concerning these composites is their weathering durability. In this study, the effects of two ultraviolet absorbers (UVAs), UV-326 and UV-531, on the durability of rice-hull/high-density polyethylene (HDPE) composites were evaluated after the samples were exposed to UV-accelerated weathering tests for up to 2000 h. All of the samples showed significant fading and color changes in exposed areas. X-ray photoelectron spectroscopy and Fourier transform infrared spectroscopy were used to detect surface chemical changes. The results indicate that surface oxidation commenced immediately within the first 500 h of exposure for all of the samples. However, the control rice-

hull/HDPE composites underwent a greater degree of oxidation than those with the UVAs. Scanning electron microscopy revealed that the rice-hull/HDPE composites degraded significantly upon accelerated UV aging, with dense cracking on the exposed surface. The UVAs provided effective protection for the rice-hull/HDPE composites, and UV-326 had a more positive effect on the color stability than UV-531. The results reported herein serve to enhance our understanding of the efficiency of UV stabilizers in the protection of rice-hull/HDPE composites against UV radiation, with a view toward improving their formulation.  
© 2012 Wiley Periodicals, Inc. *J Appl Polym Sci* 000: 000–000, 2012

**Key words:** ageing; composites; degradation; polyethylene (PE)

## INTRODUCTION

Natural-fiber-reinforced polymer composites have been increasingly accepted as building materials and have advantages of low maintenance, high durability, and environmental friendliness. These products are often used in exterior applications, for example, in decks and garden furniture. In North America, where the use of these products has flourished, wood flour (pine, maple, and oak flours with mesh sizes between 20 and 100 mesh), as the most widely used natural-fiber component, is typically incorporated into wood/plastic composites at 50–60 wt %.<sup>1</sup> However, the use of greater quantities of agricultural plant fibers to reinforce polymers has been paid much attention in recent years. For example, in China, most manufacturers use rice-hull powder as the fiber component because it is an agricultural res-

idue that is easily obtained and because its cost is much lower than that of wood fibers (WFs).

However, with rapid growth in the outdoor use of natural-fiber-reinforced polymer composites,<sup>2–8</sup> it was found that these products are susceptible to color changes and a loss of mechanical properties during long-term outdoor applications. Thus, the durability of these products against weathering, particularly against UV light, has become a widespread concern.

Some research groups have addressed changes in the color and surface chemistry and the loss of mechanical properties after weathering.<sup>1,7–12</sup> It has been shown that the manufacturing method, exposure type, and addition of a photostabilization system affect the extent and rate of lightening.<sup>3–9</sup> It has been demonstrated that colorants and ultraviolet absorbers (UVAs) are effective in reducing the fading of WF/high-density polyethylene (HDPE) composites after accelerated weathering.<sup>4,6,10,13</sup> UV exposure can cause the photodegradation of both the polymer matrix and natural-fiber components of WF/polymer composites.<sup>2–7,14</sup> Photodegradation may lead to the discoloration of products. Furthermore, prolonged UV exposure may ultimately lead to a loss of mechanical integrity.<sup>1–3,5</sup> Lundin<sup>3</sup> weathered photostabilized WF/polyethylene (PE) composites and monitored the

Correspondence to: Q. Wang (qwwang@nefu.edu.cn).

Contract grant sponsor: NSFC; contract grant numbers: 30671644, 30771680.

TABLE I  
UVA Additive Descriptions

Property	UVA	
	Benzophenone	Benzotriazole
Trade name	UV-531	UV-326
Molecular mass (g/mol)	326	315.5
Molecular formula	C <sub>21</sub> H <sub>26</sub> O <sub>3</sub>	C <sub>17</sub> H <sub>18</sub> N <sub>3</sub> OCl
Melting point (°C)	47–49	137–141
Wavelengths absorbed (nm)	300–400	270–380

degradation of their mechanical properties. The results showed that the composites lost 33% of their stiffness after 2000 h of weathering. Stark and Matuana<sup>1,9,10</sup> used Fourier transform infrared (FTIR) spectroscopy to examine the surface chemistry changes of wood-flour-filled PE after UV weathering and also found that UVAs and colorants were the most effective photostabilizers for WF/HDPE composites.<sup>6</sup>

Most literature reports have focused on the mechanical properties of WF-reinforced polymer composites. However, the weathering resistance of rice-hull/HDPE composites has not been studied in detail. In this study, we used two types of UV stabilizers to improve the durability of rice-hull/HDPE composites and investigated in detail the changes in the chemical structure that occurred during weathering. Substituted *o*-hydroxybenzophenones (UV-531) and benzotriazoles (UV-326) act as UVAs; they prevent excitation of the polymer by absorbing UV light and converting it into heat. In other words, UVAs decompose hydroperoxide groups to nonradical products. Changes in the carbonyl groups (C=O) and cellulose C–O groups were measured with FTIR spectroscopy and X-ray photoelectron spectroscopy (XPS) to gain insight into the effectiveness of these UVAs in rice-hull/HDPE composites. The results reported here should enhance our understanding of the efficiency of UV stabilizers in the protection of rice-hull/HDPE composites against UV radiation, with a view toward improving their formulation.

## EXPERIMENTAL

### Materials

The HDPE material used in this study (density = 0.954 g/cm<sup>3</sup>, melt flow index = 0.9 g/min) was supplied by Petrification Co. (Daqing, China), and rice-hull powder (50–80 mesh) was purchased from a local farmer. The two UVAs were purchased from Beijing Specialty Chemicals Co. (Beijing, China) and their characteristics are listed in Table I and Figure 1.

### Processing

Rice-hull powder was dried at 105°C to decrease its moisture content to approximately 0.9% (dry weight

basis) before the compounding process. Composite formulations were prepared containing 0.5% (w/w) UVA (UV-531 or UV-326) and 60% (w/w) rice-hull powder, with HDPE comprising the remainder. Rice-hull powder, HDPE, and UVA additive were dry-blended at a preset temperature of 85°C in a high-intensity, 1-L kinetic mixer at 3200 rpm with a tip speed of 23 m/s. After 10 min of mixing, the mixture was discharged. Compounding and extruding were completed through a one-step extrusion process in a twin-screw/single-screw extruder system (Nanjing, China). The rotary speed of the twin-screw was 150 rpm. The processing temperatures for extrusion were set at 180°C for the melting zone, 160–170°C for the pumping zone, and 170°C for the die zone. Composites without UVAs were also prepared as controls. The cross section of the extruded lumber was 4.0 × 40.0 mm<sup>2</sup>.

### Weathering

Rice-hull/HDPE specimens with dimensions of 80 × 13.5 × 4 mm<sup>3</sup> were cut from the extruded lumber. These specimens were weathered in a Q-panel UV-aging system (American, Q-Panel Lab Products, Cleveland, USA). Accelerated weathering conditions were applied according to ASTM G 154-04, with treatment for up to 2000 h. The weathering cycle consisted of 8 h of dry UV exposure at 60°C, followed by 4 h of condensation exposure at 50°C without irradiation. Specimens were removed for analysis after 250, 500, 1000, 1500, and 2000 h of exposure and were compared with unexposed samples. The UVA 340 lamps were calibrated every 500 h.

### Scanning electron microscopy (SEM)

The surfaces of samples were sputter-coated with gold and analyzed under a scanning electron microscope (FEI Company, Hillsboro Oregon, USA) at a working distance of approximately 25 mm with a voltage of 15 kV and a probe current of 6 × 10<sup>-10</sup> A.

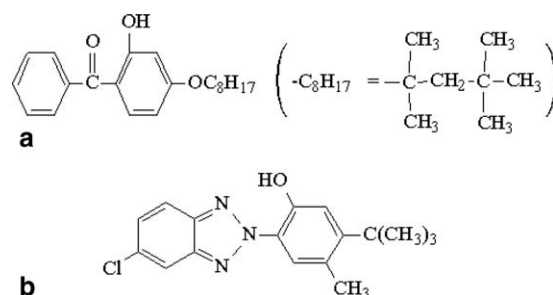


Figure 1 Chemical structures of (a) UV-531 and (b) UV-326.

### Colorimetric analysis

The surface color of the samples was measured with an NF333 photometer (Nippon Denshoku Co. Tokyo, Japan) according to the CIELAB color system. The lightness ( $L^*$ ) and chromaticity coordinates ( $a^*$  and  $b^*$ ) were measured for six replicate samples.  $L^*$  represents the lightness coordinate and varies from 100 (white) to 0 (dark).  $a^*$  represents the red ( $+a^*$ ) to green ( $-a^*$ ) coordinate, and  $b^*$  represents the yellow ( $+b^*$ ) to blue ( $-b^*$ ) coordinate. An increase in  $L^*$  means that the sample has lightened or faded (i.e., positive  $\Delta L^*$  for lightening and negative  $\Delta L^*$  for darkening). Similarly, a positive  $\Delta a^*$  represents a color shift toward red, and a negative  $\Delta a^*$  represents a color shift toward green. A positive  $\Delta b^*$  represents a color shift toward yellow, and a negative  $\Delta b^*$  represents a color shift toward blue. The total color change ( $\Delta E$ ) was calculated according to ASTM D 2244:<sup>15</sup>

$$\Delta E = [(\Delta L^*)^2 + (\Delta a^*)^2 + (\Delta b^*)^2]^{1/2}$$

It should be noted that  $\Delta E^*$  represents the magnitude of the color difference but does not indicate the direction of this difference.

### Infrared spectroscopic analysis

FTIR spectra (KBr disk method) were recorded on a MAGNA-IR560 (Nicolet Wisconsin, USA) spectrometer to obtain detailed information about the functional groups on the composite surface before and after weathering. Scanning was carried out at a resolution of  $4 \text{ cm}^{-1}$  from  $4000$  to  $400 \text{ cm}^{-1}$ . The peak intensity was determined by subtraction of the height of the baseline from the total peak height. The same baseline was chosen for each peak before and after weathering. At least five replicate specimens were analyzed for each formulation.

### XPS analysis

XPS spectra were generated with a K-Alpha spectrograph (Hewlett-Packard Development Company, Palo Alto California, USA). To determine the type of O—C bonds present, chemical bond analysis of carbon was accomplished by deconvolution of the curve into four peaks. The deconvoluted peak assignments and the corresponding binding energies and bond types are shown in Table II.

## RESULTS AND DISCUSSION

### Changes in the surface morphology

The morphologies of the exposed and unexposed surfaces of the rice-hull/HDPE composites are shown in Figure 2. With or without UVA, the specimens dis-

**TABLE II**  
Deconvoluted Peak Assignment, Binding Energy, and Bond Type for High-Resolution  $C_{1s}$  and  $O_{1s}$  XPS Data

Carbon group	Binding energy (eV)	Bond
C <sub>1</sub>	284.84	C—C or C—H
C <sub>2</sub>	286.13	C—O
C <sub>3</sub>	287.18	O—C—O or C=O
C <sub>4</sub>	288.38	O—C=O
O <sub>1</sub>	531.71	C=O
O <sub>2</sub>	533.28	O—C—O

played a smooth and integrated surface before weathering [Fig. 2(a,d,g)]. After exposure to UV weathering for 500 h, specimens without UVAs showed cracks and exposed rice-hull particles on the surface [Fig. 2(b)]. These cracks became increasingly extensive with increasing UV weathering duration [Fig. 2(c)]. However, the specimens containing UVAs displayed only tiny cracks on their surfaces during the first 500 h of accelerated UV weathering [Fig. 2(e,h)]. Although all of the cracks tended to enlarge during weathering [Fig. 2(c,f,i)], the composites containing UVAs showed fewer cracks on their surfaces than those without UVAs. This demonstrates that the UVAs effectively protected rice-hull/HDPE composites against damage by UV radiation. However, this protection was limited, and the rice-hull/HDPE surfaces ultimately cracked when exposed to UV weathering for a sufficiently long time.

The melting point of UV-326 is higher than that of UV-531 (Table I). The former retains its crystallinity at extrusion temperatures. Compared to the specimens containing UV-531, those with UV-326 showed less cracking and maintained much better surfaces, even at the end of 2000 h of testing. UV-326 probably absorbed more UV light compared to UV-531. It was also found by SEM that crystals appeared on the surface of the specimen with UV-326 after 500 h of UV weathering [Fig. 2(h)]. Microanalysis by SEM-energy dispersive spectroscopy (EDS) [Fig. 2(j)] proved that these crystals contained Cl and indicated that they consisted of UV-326. The UV-326 powder was enveloped in the HDPE matrix. Upon exposure to UV weathering, the particles tended to migrate to the surface. With prolonged exposure, the UV-326 crystals were gradually washed away by condensed water or consumed, and so their protective function against weathering was slowly lost. As a result, the surface of the rice-hull/HDPE composite cracked.

### Changes in the surface color

The rice-hull/HDPE composites, with or without UVA, faded during accelerated UV weathering (Fig. 3).  $L^*$  increased most sharply during the first 500 h of exposure, and then, further increases became less pronounced. Samples containing UVA clearly

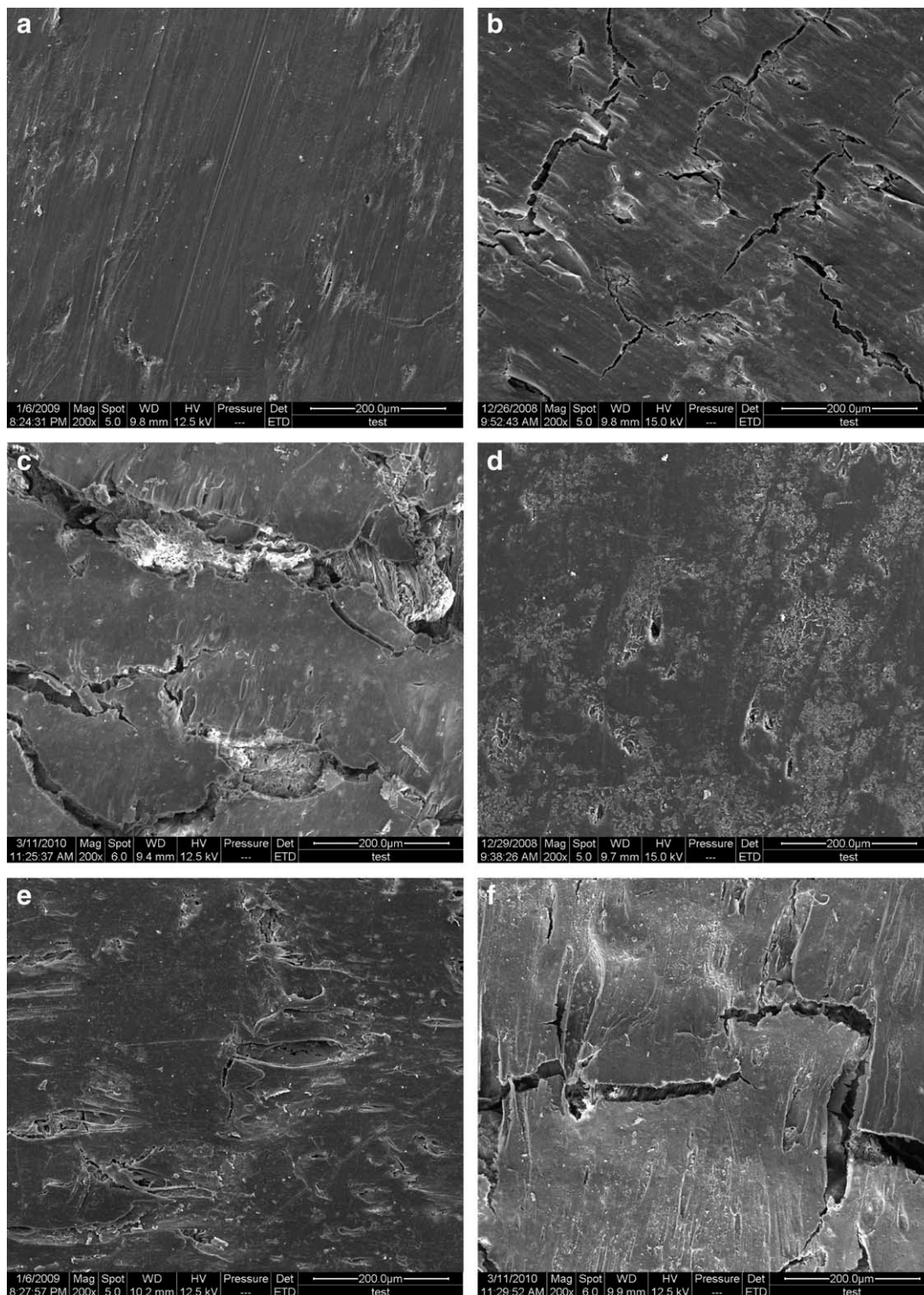


**Figure 2** SEM images and EDS analysis of rice-hull/HDPE composites before and after UV weathering. Samples (a) without UVA before weathering, (b) without UVA after weathering for 500 h, (c) without UVA after weathering for 2000 h, (d) with 0.5% UV-531 before weathering, (e) with UV-531 after weathering for 500 h, (f) with UV-531 after weathering for 2000 h, (g) with 0.5% UV-326 before weathering, (h) with UV-326 after weathering for 500 h, and (i) with UV-326 after weathering for 2000 h. (j) Elemental microanalysis (SEM-EDS) of the sample with UV-326 after weathering for 500 h. [Color figure can be viewed in the online issue, which is available at [wileyonlinelibrary.com](http://wileyonlinelibrary.com).]

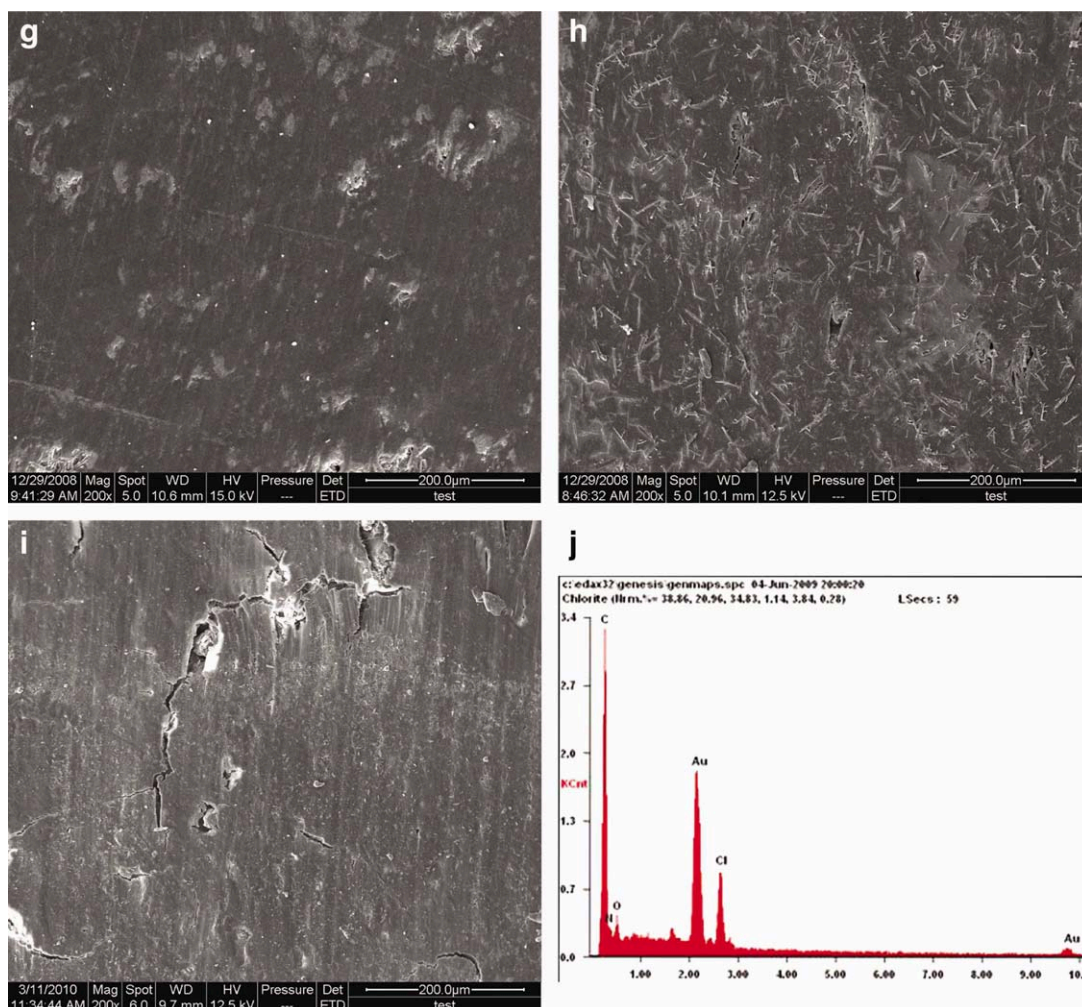


Figure 2 (Continued)

showed less lightening than those without UVA. The incorporation of UV-326 resulted in significantly smaller changes in  $L^*$  compared to that of UV-531, which meant less fading.

Stark and coworkers<sup>5,13</sup> reported that wood-plastics composites (WPC) lightening could be attributed to the chain scission of HDPE and its migration to

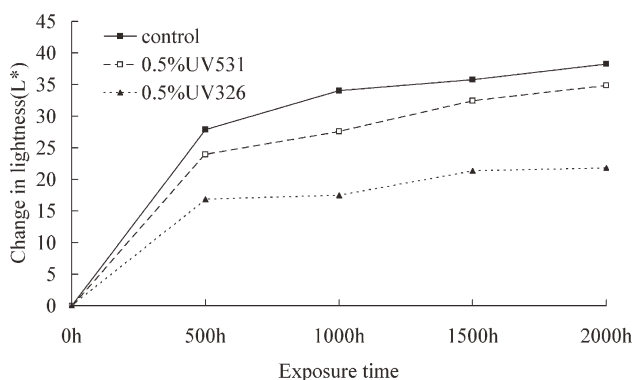


Figure 3 Change in the lightness of the rice-hull/HDPE composites after accelerated UV weathering for 2000 h.

the surface and to the photobleaching of lignin. In this study, it was presumed that UVA could inhibit lightening by absorbing some UV radiation; this resulted in less UV radiation being available to bleach the samples.<sup>16</sup>

The percentage changes in  $L^*$  for all of the formulations after 2000 h of UV exposure are listed in Table III. On the basis of the unexposed specimens, the  $L^*$  values of the control specimens increased by 91.8%, whereas  $L^*$  of specimens with UV-326 and UV-531 increased by 50.89 and 82.05%, respectively. Thus, UV-326 provided the least fading. This result means that UV-326 was more efficient in protecting the composite than UV-531; this was consistent with

TABLE III  
 $\Delta L^*$  of the Photostabilized 60% Rice-Hull-Filled HDPE Composites after UV Weathering

Formulation	$\Delta L^*$
Control	91.80
0.5% UV-531	82.05
0.5% UV-326	50.89

**TABLE IV**  
Peak Wave Numbers for the FTIR Analysis and the Corresponding Functional Groups and Vibration Types<sup>11–16,19,20</sup>

Wave number (cm <sup>-1</sup> )	Functional group	Vibration
2917 or 2850	—CH <sub>2</sub> —	C—H stretching
1700–1750	R(C=O)OH	C=O stretching
1650–1690	C=O (conjugated)	C=O stretching conjugated with benzene
1507	Aromatic ring	Ring stretching of the aromatic ring framework
1635–1599	C=N (conjugated)	C=N stretching conjugated with benzene
1470 or 1460	—CH <sub>2</sub> —	C—H bonding, crystalline or amorphous
1060–1095	C—O(H)	C—O stretching or deformation
730 or 720	—CH <sub>2</sub> —	C—H rocking, crystalline, or amorphous

the SEM observation. More stable UV-326 emerged on the surface of the rice-hull/HDPE composite than unstable UV-531 and provided more protection.

### Changes in the surface chemistry observed by infrared spectroscopy

FTIR spectroscopy was used to study the chemical changes on the surface of rice-hull/HDPE composites before and after weathering. The salient FTIR peaks and the corresponding groups and vibration types are listed in Table IV. The FTIR spectra of rice-hull powder, HDPE, and unweathered rice-hull/HDPE composites are shown in Figure 4. The typical absorbance peaks of UV 531 and UV 326 are shown in Figure 5.

The intensities of the peaks at  $\nu = 1715$  and  $1095$  cm<sup>-1</sup>, which represent carbonyl (C=O) stretching

and C—O stretching, respectively, mainly in cellulose and hemicellulose<sup>11,17–19</sup> of the rice-hull powder, were measured. The carbonyl index and fiber index were calculated according to the following equations:<sup>9,18</sup>

$$\text{Carbonyl index} = \frac{I_{1715}}{I_{2912}} \times 100$$

$$\text{Fiber index} = \frac{I_{1095}}{I_{2912}} \times 100$$

where  $I$  denotes the peak intensity. The peak intensity was normalized to the peak at  $\nu = 2912$  cm<sup>-1</sup>, which corresponds to alkane C—H stretching vibrations of methylene (—CH<sub>2</sub>—) groups. This peak was chosen as a reference because it changed the least during weathering.

The FTIR spectra for all of the rice-hull/HDPE composites were clearly different before and after accelerated UV weathering (Figs. 6–8). The peak at  $\nu = 1700$ – $1750$  cm<sup>-1</sup>, corresponding to C=O stretching, increased in intensity after 500 h of weathering; this indicated that surface oxidation occurred in the first 500 h of exposure. The spectral region of  $\nu = 1097$ – $1060$  cm<sup>-1</sup>, which is associated with C—O stretching in cellulose and hemicellulose,<sup>12,18,19</sup> showed very high intensities for the control and UV-326 samples before weathering, but these signals significantly decreased after UV weathering for 2000 h (Figs. 6–8); this indicated losses of cellulose and hemicellulose at the composite surface. The peaks around  $\nu = 1650$  and  $1507$  cm<sup>-1</sup>, attributable to aromatic ring framework stretching in lignin, disappeared after UV exposure of just 500 h (Figs. 6 and 8); this indicated photodegradation of the aromatic lignin structure. Changes in the carbonyl index and fiber index are shown in Figures 10 and 11.

Narrow bands at  $\nu = 1686$  and  $1062$  cm<sup>-1</sup> could be attributed to stretching vibrations of the conjugated carbonyl group C=O and C—O in UV-531,

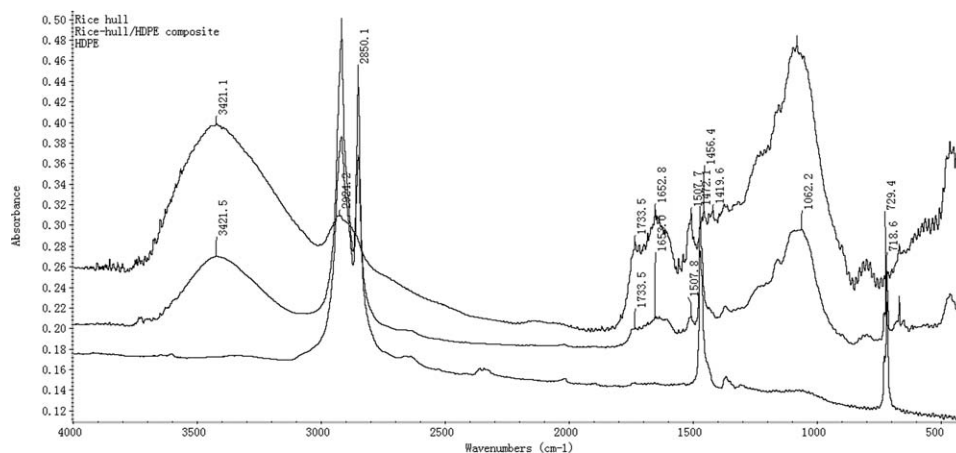


**Figure 4** FTIR spectra of the rice powder, rice hull/HDPE, and HDPE.

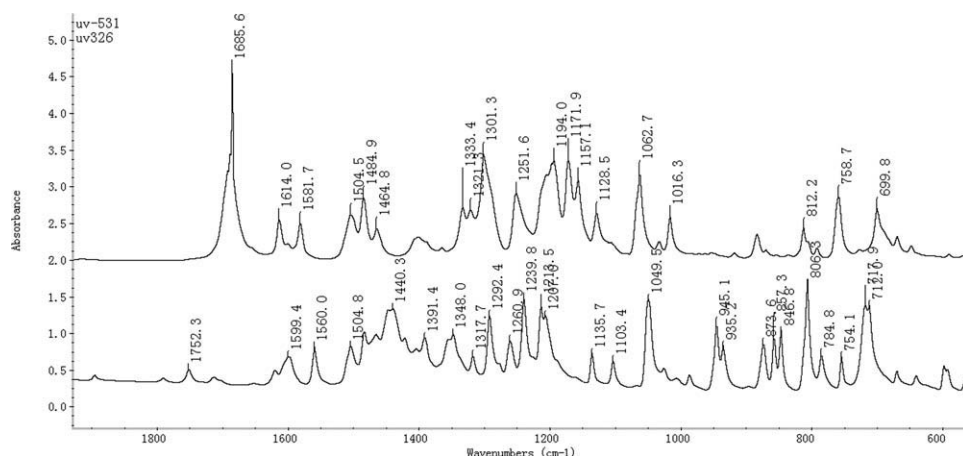


Figure 5 FTIR spectra of UV-531 and UV-326.

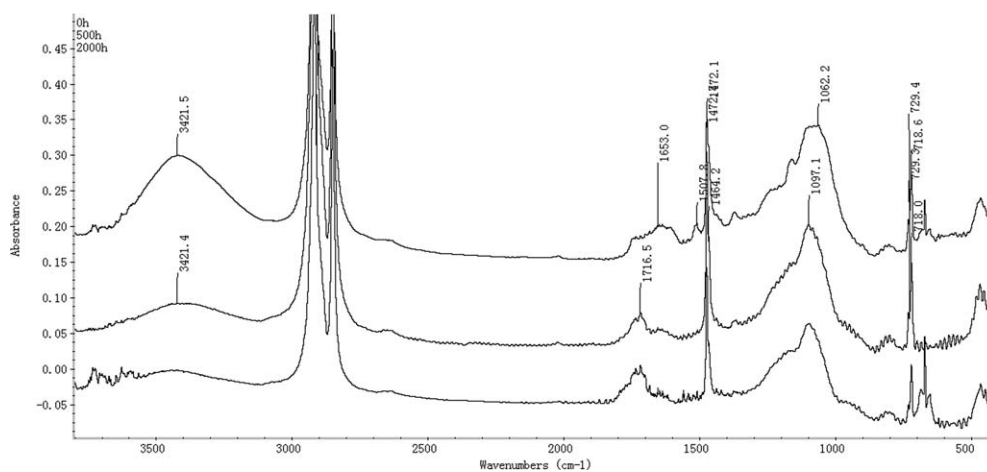


Figure 6 FTIR spectra of the rice-hull/HDPE composites before and after weathering.

respectively (Fig. 5). These peaks were very intense before weathering but almost disappeared after UV exposure for 2000 h. The peak around  $\nu = 1635\text{--}1599\text{ cm}^{-1}$  corresponded to the characteristic absorption

of the conjugated imino group  $\text{C}=\text{N}$  in UV-326, and this feature was greatly decreased after 2000 h of UV exposure. The results indicate that the UVAs (UV-531 and UV-326) on the surfaces of the samples

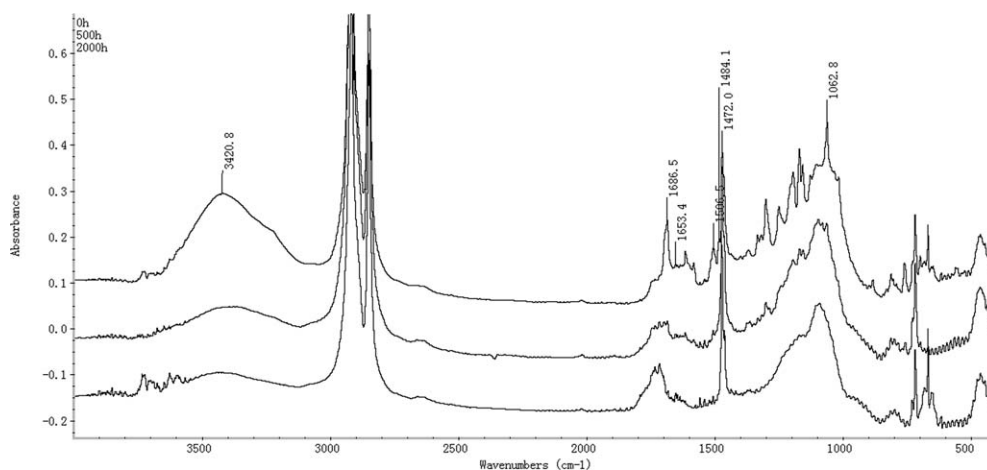
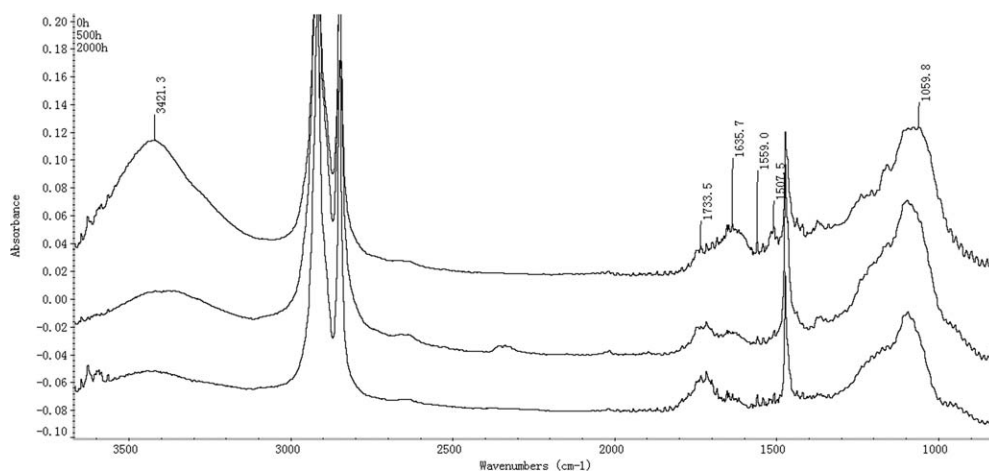


Figure 7 FTIR spectra of the rice-hull/HDPE composites with UV-531 before and after weathering.



**Figure 8** FTIR spectra of the rice-hull/HDPE composites with UV-326 before and after weathering.

were consumed. Substituted *o*-hydroxybenzophenones (UV-531) and benzotriazoles (UV-326) absorbed UV and transferred inside the molecules on the basis of reversible processes (Fig. 9). Then, the created heat energy in this process was released.<sup>20</sup>

### Carbonyl group formation

The carbonyl index of the control sample increased for up to 1000 h of exposure and then decreased (Fig. 10). The largest increases in the carbonyl index occurred during the first 500 h of exposure. The increase in the carbonyl group index for PE after weathering is known to be proportional to the number of chain scissions that occur therein.<sup>1,9,10</sup> Therefore, the results indicate that chain scission may have occurred immediately upon UV exposure and that the number of chain scissions increased with increasing exposure time. At the same time, chain scission decreased the density of entanglements in the amorphous phase and allowed shorter molecules to migrate to the sample surface,<sup>9,10</sup> which may have resulted in WPC lightening. SEM showed that weathering caused more severe cracks, and more

fractured rice-hull powder particles appeared on the surfaces of the control samples. Fractured and loose rice-hull powder particles might have been washed away during the condensation cycles; this decreased the amount of degraded rice-hull powder and plastic on the outer surface and resulted in a decrease in the carbonyl index of the control samples after 1000 h of exposure. This result was consistent with that of James and coworkers.<sup>14,21</sup> They also found that the carbonyl content of WPC increased during the initial stage of UV weathering and finally decreased after a certain duration of exposure.

The carbonyl indices of the samples containing UVAs also increased with the exposure time. However, the increment was less than that of the control sample during exposure. These results demonstrate that the UVAs partly absorbed UV light and effectively decreased the oxidation of samples due to UV exposure.

Samples containing UV-326 exhibited the smallest increment in the carbonyl index of all of the samples, possibly because of the transfer of UV-326 crystals to the surface after 500 h of UV weathering (Fig. 2), with this additive absorbing more UV light

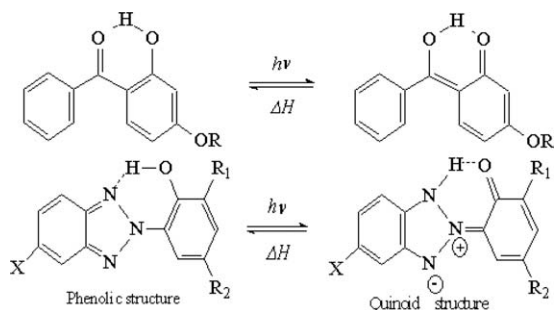


**Figure 9** Phenolic structure and quinone structure reversible processes inside the molecules of the UVAs.  $h\nu$ -absorb UV-light,  $\Delta H$ -emit heat energy.

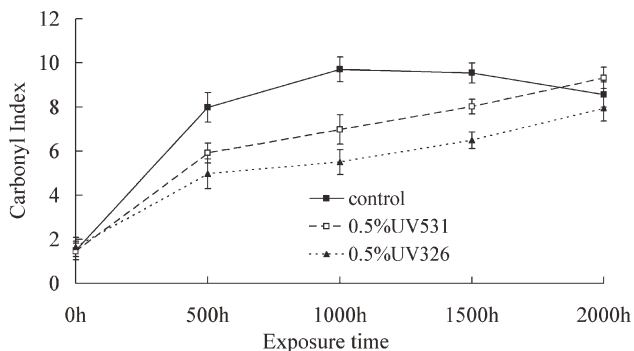


**Figure 10** Change in the carbonyl index of the rice-hull/HDPE composites after accelerated weathering for 2000 h. Each data point represents the average of five samples, and the error bars represent one standard deviation.



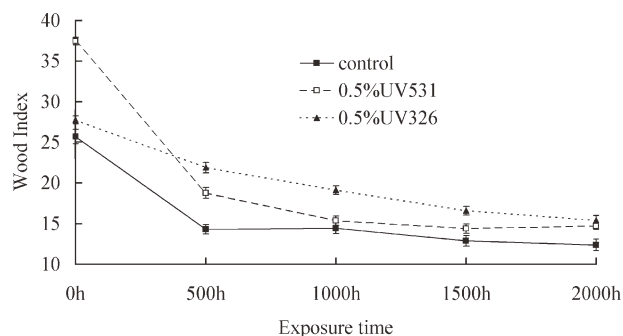


**Figure 11** Change in the wood index of the rice-hull/HDPE composites after accelerated weathering for 2000 h. Each data point represents the average of five samples, and the error bars represent one standard deviation.

than UV-531. Hence, UV-326 was more effective in protecting the rice-hull/HDPE composites from UV weathering than UV-531. The control sample did not differ in the carbonyl index from samples containing UV-531 at the end of 2000 h of weathering. This indicated that UV-531 was not effective in protecting the plastic from photodegradation after long-term UV exposure because it was consumed.

### Changes in the fiber index

The fiber indices of the rice-hull/HDPE composites containing UVAs were higher than that of the control sample before weathering (Fig. 11). The UVAs themselves had C—O groups, which resulted in a higher fiber index of the corresponding composite (Figs. 7 and 8).

It has been reported<sup>22,23</sup> that the photodegradation of wood can be attributed to degradation of its components, namely, cellulose, hemicellulose, lignin, and extractives. Thus, changes in the wood index could be considered indications of photodegradation. The wood indices of all of the samples decreased with increasing exposure time (Fig. 11); this indicated the occurrence of rice-hull photodegradation on the composite surfaces. It was very likely that weathering caused the appearance of microcracks on the

surface of the rice-hull/HDPE composites; this allowed the penetration of more UV radiation and the permeation of moisture and resulted in photodegradation of interior cellulose and lignin.<sup>1</sup>

The wood indices of all of the samples decreased most rapidly during the first 500 h of exposure, and thereafter, the decrease became less pronounced. Samples containing UVA had higher wood indices than the control sample after 2000 h of weathering, and samples containing UV-326 had the highest wood indices. This was consistent with the SEM observation that samples containing UVA showed fewer cracks on their surfaces and that the sample incorporating UV-326 showed fewer cracks after 2000 h of UV exposure.

### Changes in the elemental content and valence state on the surfaces of the composites

The results of the surface elemental analysis of the rice-hull/HDPE before and after UV weathering as obtained by XPS are listed in Table V. The main elements detected were oxygen and carbon. The O/C atomic ratio was calculated as an indication of surface oxidation. The XPS data listed in Table V show an increase in the total number of oxygenated carbon bonds. Thus, after 2000 h of weathering, the O/C ratio increased for all of the samples; this indicated that the surfaces of all of the samples were oxidized.

The C1s peak was separated by deconvolution into four subpeaks, C<sub>1</sub>, C<sub>2</sub>, C<sub>3</sub>, and C<sub>4</sub>. The theoretical binding energies and corresponding bond types are shown in Table II. The C<sub>1</sub> peak did not correspond to a C—O bond, whereas the C<sub>2</sub>, C<sub>3</sub>, and C<sub>4</sub> peaks did. The ratio of oxidized to unoxidized carbon (C<sub>ox/unox</sub>) was also calculated as follows:

$$C_{\text{ox/unox}} = \frac{C_{\text{oxidized}}}{C_{\text{unoxidized}}} = \frac{C_2 + C_3 + C_4}{C_1}$$

A decrease in the C<sub>1</sub> peak intensity indicated a decrease in the concentration of unoxidized carbon

**TABLE V**  
Relative Quantities of Various Carbon–Oxygen Bonds in the Control and Rice-Hull/HDPE Samples Containing UVAs as Determined by XPS

	C <sub>1</sub>	C <sub>2</sub>	C <sub>3</sub>	C <sub>4</sub>	O <sub>1</sub>	O <sub>2</sub>	O/C	C <sub>ox/unox</sub>
Control sample								
Unweathered sample	80.52	7.89	3.83	0.67	4.13	2.96	0.076	0.154
Sample weathered for 2000 h	50.18	24.07	4.83	1.78	16.28	3.98	0.254	0.589
Sample with UV-531								
Unweathered sample	71.55	10.55	5.93	1.57	3.91	6.49	0.116	0.252
Sample weathered for 2000 h	56.59	16.38	6.65	3.99	11.68	4.71	0.196	0.477
Sample with UV-326								
Unweathered sample	78.16	10.82	1.83	1.24	4.01	3.94	0.086	0.178
Sample weathered for 2000 h	60.02	14.01	3.59	3.55	13.92	4.91	0.511	0.352

atoms. Increases in  $C_2$  and  $C_3$  were observed after weathering. On the other hand, weathering significantly increased  $C_{ox/unox}$  for all of the samples (Table V); this implied that significant surface oxidation occurred after 2000 h of exposure. The XPS results were consistent with the FTIR results.

Stark and Matuana<sup>1,9</sup> found that weathering significantly increased  $C_{ox/unox}$  for both the neat HDPE and WF/HDPE composites; this proved that substantial surface oxidation occurred after 2000 h of exposure. The increase in  $C_{ox/unox}$  for both the neat HDPE and WF/HDPE composites appeared to be mainly due to an increase in the number of hydroxyl groups (i.e., an increase in  $C_2$ ). In addition, surface oxidation due to weathering was more pronounced for the WF/HDPE composite samples than for the pure HDPE. In this study,  $C_{ox/unox}$  increased dramatically for the rice-hull/HDPE composites after weathering (it increased by more than 89%, compared to 5% for the pure HDPE samples); this suggested that the addition of rice-hull powder to the HDPE matrix accelerated surface photooxidation. However, there was no significant difference in the increase in  $C_{ox/unox}$  between UV-531 and UV-326.

### CONCLUSIONS

The weathering of rice-hull/HDPE composites was investigated. XPS analysis revealed that surface oxidation of all samples occurred after 2000 h of exposure. The rice-hull/HDPE composites without UVAs showed surface discoloration after UV weathering as a consequence of extensive chemical degradation involving chain-scission reactions and the formation of carboxyl groups. On the basis of less surface discoloration, a smaller change in the carbonyl index, and a higher fiber index than the other counterparts with increasing exposure time, the sample with UV-326 was considered to have shown the least photodeterioration.

Surface cracks were apparent for all of the rice-hull/HDPE composites; this reflected significant degradation after 2000 h of UV exposure. However,

cracks in the composites containing UVAs appeared to be less severe than in those without UVAs. The UVAs protected the rice-hull/HDPE composites from UV degradation to a certain extent, with UV-326 being more effective than UV-531.

### References

1. Stark, N. M.; Matuana, L. M. *Polym Degrad Stab* 2007, 92, 1.
2. Joseph, K.; Thomas, S.; Pavithran, C. *Compos Sci Technol* 1995, 53, 99.
3. Lundin, T. M.S. thesis, University of Wisconsin—Madison, 2001.
4. Falk, R. H.; Lundin, T.; Felton, C. In *Proceedings: The PATH Conference on Durability and Disaster Mitigation in Wood-Frame Housing*; Madison, 2000, p 175.
5. Stark, N. M.; Matuana, L. M. *Proc Annu Tech Conf* 2002, 2, 2209.
6. Stark, N. M.; Matuana, L. M. *J Appl Polym Sci* 2003, 90, 2609.
7. Matuana, L. M.; Kamdem, D. P.; Zhang, J. *J Appl Polym Sci* 2001, 80, 1943.
8. Matuana, L. M.; Kamdem, D. P. *Polym Eng Sci* 2002, 42, 1657.
9. Stark, N. M.; Matuana, L. M. *Polym Degrad Stab* 2004, 86, 1.
10. Stark, N. M.; Matuana, L. M. *J Appl Polym Sci* 2004, 94, 2263.
11. James, S. F.; Armando, G. M.; Michael, P. W.; Peter, R. G. *Polym Degrad Stab* 2008, 93, 1405.
12. Colom, X.; Canavate, J.; Pages, P.; Saurina, J.; Carrasco, F. *J Reinf Plast Compos* 2000, 19, 818.
13. Muasher, M.; Sain, M. *Polym Degrad Stab* 2006, 91, 1156.
14. Du, H.; Wang, W. H.; Wang, Q. W.; Zhang, Z. M.; Sui, S. J.; Zhang, Y. H. *J Appl Polym Sci* 2010, 118, 1068.
15. *Annual Book of ASTM Standards*; American Society for Testing and Materials: Conshohocken, PA, 2001; p 8.02.
16. Stark, N. M.; Matuana, L. M. *Polym Degrad Stab* 2006, 91, 3048.
17. Pandey, K. K.; Vuorinen, T. *Polym Degrad Stab* 2008, 93, 2138.
18. Stark, N. M.; Matuana, L. M.; Clemons, C. M. *J Appl Polym Sci* 2004, 93, 1021.
19. Colom, X.; Carrillo, F.; Nogues, F.; Garriga, P. *Polym Degrad Stab* 2003, 80, 543.
20. Pospisil, J.; Nespurek, S. *Prog Polym Sci* 2000, 25, 1261.
21. James, S. F.; Armando, G. M.; Michael, P. W.; Peter, R. G. *Polym Degrad Stab* 2008, 93, 1405.
22. Heitner, C. In *Photochemistry of Lignocellulosic Materials*; ACS Symposium Series 531; American Chemical Society: Washington, DC, 1993; p 3.
23. Hon, D. N. S. *Weathering and photochemistry of wood*. In: Hon, D.N.S.; Shiraishi, N. editors. *Wood and cellulosic chemistry*. New York: Marcel Dekker, 2000, 2:512–546.